ELSEVIER

Contents lists available at ScienceDirect

## Fire Safety Journal

journal homepage: www.elsevier.com/locate/firesaf





# Enhancing foam fire suppression analysis through CO<sub>2</sub> TDLAS quantification

Katherine M. Hinnant a, \*, Spencer L. Giles A, Ramagopal Ananth A, J. Houston Miller

- <sup>a</sup> Chemistry Division, U.S. Naval Research Laboratory, Washington, DC, USA
- <sup>b</sup> George Washington University, Washington, DC, USA

#### ARTICLE INFO

Keywords: Spectroscopy Diode laser Fire suppression Aqueous foam Surfactants

#### ABSTRACT

Tunable diode laser absorption spectroscopy (TDLAS) was used to monitor  $CO_2$  concentrations above a pool fire as experimental firefighting foams were applied to the pool surface. A  $2.0~\mu m$  diode laser was used in a modified section of ventilation duct above a 19~cm diameter heptane pool fire. Laser signal intensity and temperature were measured to calculate  $CO_2$  concentration with time. The concentration profiles were determined for a reference fluorosurfactant foam and a series of fluorine-free foams containing siloxane surfactants blended with a hydrocarbon surfactant (Glucopon 215 UP), and solvent. Seven mixtures were evaluated: three foams fully covered the fuel pool and two foams extinguished the fire. Due to the rapid response of the measurement technique, a dramatic drop in  $CO_2$  concentration was observed as the fire was extinguished. Pool coverage corresponded to an observed peak in  $CO_2$  concentration. The concentration profiles allowed for a more accurate assessment of foams that were unable to extinguish a pool fire. Further analysis of these profiles may elucidate time-scales important for rapid fire suppression. Defining and characterizing mechanisms of foam fire suppression at these time-scales may improve and accelerate research efforts for the development of fluorine-free surfactants in firefighting foams.

## 1. Introduction

Aqueous film forming foams (AFFF) are effective at suppressing Class B liquid pool fires, but contain environmentally-harmful fluorinated surfactants [1,2]. Researchers aim to identify environmentally-friendly surfactant alternatives with matched fire extinction performance. Alternative surfactants/formulations have been proposed based on mechanisms related to their low surface tension abilities [3,4] (siloxane surfactants [5–8] specifically) or their improved foam stability (increased solution viscosity to reduce liquid drainage through the foam [9,10]). These various alternatives target different proposed mechanisms of foam fire extinction, considered important for rapid pool fire suppression.

As new materials are proposed and evaluated, we not only want to understand differences in final extinction performance, but differences throughout the extinction process. Tracking foam extinction progress may elucidate time-scale differences during fire suppression or may define alternative suppression mechanisms, relevant for continued research into firefighting foams. Defining a relationship between surfactant structure or foam composition and a key mechanism may be

easier than defining a relationship directly between surfactant structure and extinction performance.

Previous experiments have tracked foam fire extinction progress through thermocouples, IR imaging [11], and heat flux gauges above a pool fire [12,13]. Xu et al. [11] used a thermocouple rake above a burning oil fire and an infrared camera to monitor the extinction process of AFFF in a compressed air foam system (CAF) at different expansion ratios. Thermal imaging revealed a spike in flame temperature after 2 s of foam application, attributed to an increase in total pressure at the flame interface due to vaporized water droplets from the foam. However, the authors do not provide comparative data between foams or trials. Rie et al. [12] and Wang et al. [13] both used a thermocouple rake and heat flux gauges to study CAF generated AFFF. Rie noted differences in proposed extinction time based on the time to temperature minimization and heat flux minimization; however, they do not provide the observed extinction time during the experiments. Wang observed spikes in temperature and heat flux as foam was introduced to the pool surface (similar to Xu et al. [11]). Temperature data taken for two fuel pool depths showed that the temperature continued to decrease after the time of extinction. In comparison, the heat flux for the deeper fuel pool

E-mail address: Katherine.hinnant@nrl.navy.mil (K.M. Hinnant).

<sup>\*</sup> Corresponding author.

reached a steady-state at the time of extinction, but for the shallower pool, the heat flux rate continued to decrease past the time of extinction. This suggests a potential lag in data collection between thermocouples, heat flux gauges, and the extinction experiment.

Although commonly used to measure combustion products, gaseous species detection has not been widely applied to measure foam fire extinction. Oxygen consumption calorimetry measures the total volumetric flow of gaseous exhaust along with the oxygen concentration in that exhaust stream to calculate the heat release rate (HRR). HRR is an important metric for characterizing material fire hazard and has therefore been extensively studied using cone calorimetry [14–16]. Equations used to calculate the HRR have been modified to include  $\rm CO_2$  and  $\rm CO$  measurements to account for incomplete combustion, Dlugogorski et al. [17] have also demonstrated that modified equations are valid even in the presence of excess water vapor that may be introduced in a fire suppression scenario with water mist.

HRR calculations from gaseous species detection have produced time resolved data during a fire event; however HRR measurements require significant instrumentation due to the sensitivity of oxygen analyzers. Cone calorimeters are commercially available for HRR measurements and are equipped with extensive instrumentation[15–17]. Blowers ensure that all exhaust gas generated is analyzed. Scrubbing systems are needed to cool down and remove water and soot from the gaseous stream to ensure accurate oxygen sensing, which introduces a significant time lag for many systems. Additionally cone calorimeter sensors often require frequent calibration to minimize drift and error in measurement as the oxygen analyzer must differentiate oxygen depletion in a small range from 21 to 18%.

While measurements of  $CO_2$  alone cannot be used to define HRR, it is a major product of combustion and has been measured through various techniques for ambient and flame environments [18–23]. One type of laser based technique is tunable diode laser absorption spectroscopy (TDLAS) which has been used to probe gaseous species concentrations close to flame environments [16] and in flame exhaust [17] using diode lasers. These measurements rely on laser light that will be optically absorbed by  $CO_2$ , creating a change in signal intensity that can be related to the concentration of  $CO_2$  across the laser path. Distributed feedback diode lasers produce a small range of wavelengths (1–2 nm) based on an applied current and temperature and can produce a signal response in  $10,000^{th}$  of a second or faster. The small wavelength range limits the likelihood of interfering gaseous species and can be chosen to maximize interactions with  $CO_2$ .

In this work, a CO<sub>2</sub> TDLAS sensor was designed to operate above a 19 cm heptane pool fire and collected data during foam application and fire extinction. Our main goal was to discriminate different foam formulations by developing a method to measure the percent fire extinction versus time profile in a more precise manner than a visual observation when 100% of the fire is extinguished. When a foam is applied on to a pool fire, concentrations of combustion products in the exhaust gases decrease with time due to fire suppression. We hypothesized that differentiations in foam fire extinction performance could be quantified using a single gas concentration if the concentration could be resolved at fine time scales. CO<sub>2</sub> was chosen as the analyzed gas over O<sub>2</sub> in order to minimize required instrumentation, and H2O due to its presence in the foam. CO was another possibility, and may be studied in the future; however, we had concerns about the absorbance signal if small concentrations of CO were produced. Consistency between trials and foams was demonstrated through a background CO2 signal and a preburn before foam application. CO2 absorbance was collected concurrently with temperature in order to accurately fit the collected absorbance data for concentration. Data were collected for a series of seven surfactant mixture foams: six experimental formulations containing different siloxane surfactants and one containing a fluorinated surfactant.

#### 2. Methodology

#### 2.1. Stack set up

Extinction performance was assessed using a 19 cm heptane pool fire, the design of which has been detailed by Ananth et al. [7]. A 19 cm diameter borosilicate glass container was filled with water leaving a 2 cm head space in the container. A 1 cm layer of heptane was then poured onto the surface, leaving a 1 cm headspace in the container for foam accumulation. A sparged foam generator with a liquid leveling system was used to generate the foam. The air flow rate used to generate foam was controlled using an Alicat flow controller at a flow rate of 1000 ml/min. To quantify  $\rm CO_2$  concentration during the extinction event, a 31 cm in length, 10 cm in diameter cylindrical section of ventilation hood above the pool fire experiment was removed and modified. A schematic of the modified hood and images of its placement relative to the pool fire can be seen in Fig. 1.

The section of hood was modified with four, bored-through 1/16'' to 1/8'' stainless steel Swagelok unions, welded in an "X" pattern around the hood to hold 4 Super OMEGACLAD<sup>TM</sup> XL Thermocouple Probes (0.125'') sheathed diameter Type K Probe) for temperature analysis. Due to extensive sooting during the experiment and the need to clean probes after each test, only 1 thermocouple was used. The other 3 ports were closed with capped Swagelok fittings during testing. The thermocouple was positioned roughly 5 cm within the hood to monitor gas temperatures close to the laser light path.

The modified hood was made optically accessible using KF25 stainless steel half-nipple fittings welded to either side of the hood. The ports were closed using KF25 quick connect stainless steel Cajon fittings with  $1^{\prime\prime}$  wedged CaF2 windows. The windows were secured to the Cajon fitting using hand cut 1/4 'neoprene gaskets on either side of the window. The window fittings were connected to the hood via KF25 fluorocarbon stainless steel O-rings, tightened with a KF24 machined clamp. Each window fitting had two 1/4 's Swagelok unions welded,  $90^\circ$  degrees from each other, onto them. These ports were used to sweep nitrogen across the windows to reduce soot accumulation. Nitrogen was swept across each port at a flow rate of 100 ml/min which represents a very small portion of the total flow pulled into the ventilation system (measured with an anemometer to be 1840 L/min). The modified hood was secured to the ventilation system using flanges, copper gaskets, and stainless steel tape around both ends.

We found that the hood system above this pool fire experiment did not pull in all exhaust gases. Hood flow had been selected to reduce experimentalist exposure to exhaust gases while ensuring the flame was not disturbed by excess flow. Observation of soot accumulation around the exterior of the hood closest to the pool fire demonstrated that not all exhaust was entering the hood. We therefore measured partial  $CO_2$  concentrations within the hood and not  $CO_2$  concentration of the total exhaust. We expect exhaust deficiencies to be consistent between trials and foams and still provide an accurate measurement of the decline in  $CO_2$  concentration with time caused by fire suppression. This allows us to compare extinction performance between foams although we cannot use the  $CO_2$  concentrations for HRR calculations or burn efficiency of individual firefighting foams.

Two breadboards were suspended around the modified hood using Unistrut hardware. On one breadboard, the diode laser output was launched onto a 2 m uncoated FC/APC fiber (P3-2000AR-2, Thorlabs) and connected to a FiberPort collimator (PAF2A-11D for AR Range 1.8–2.4  $\mu m$ , Thorlabs). Laser light was then directed onto a  $1^{\prime\prime}$  flat protected silver mirror (PF10-03-P01, Thorlabs), used to reflect laser light into the modified hood. Light passed through the stack to a  $1^{\prime\prime}$  90° off-axis gold coated parabolic mirror (MPD149-M01, Thorlabs) on a separate breadboard. The parabolic mirror focused light onto an InGaAs amplified photodetector (PDA10D2, Thorlabs) positioned 10 cm away. The detector output current through a BNC cable connected to a Texas Instruments DHPCA-100 *trans*-impedance amplifier (not pictured) in

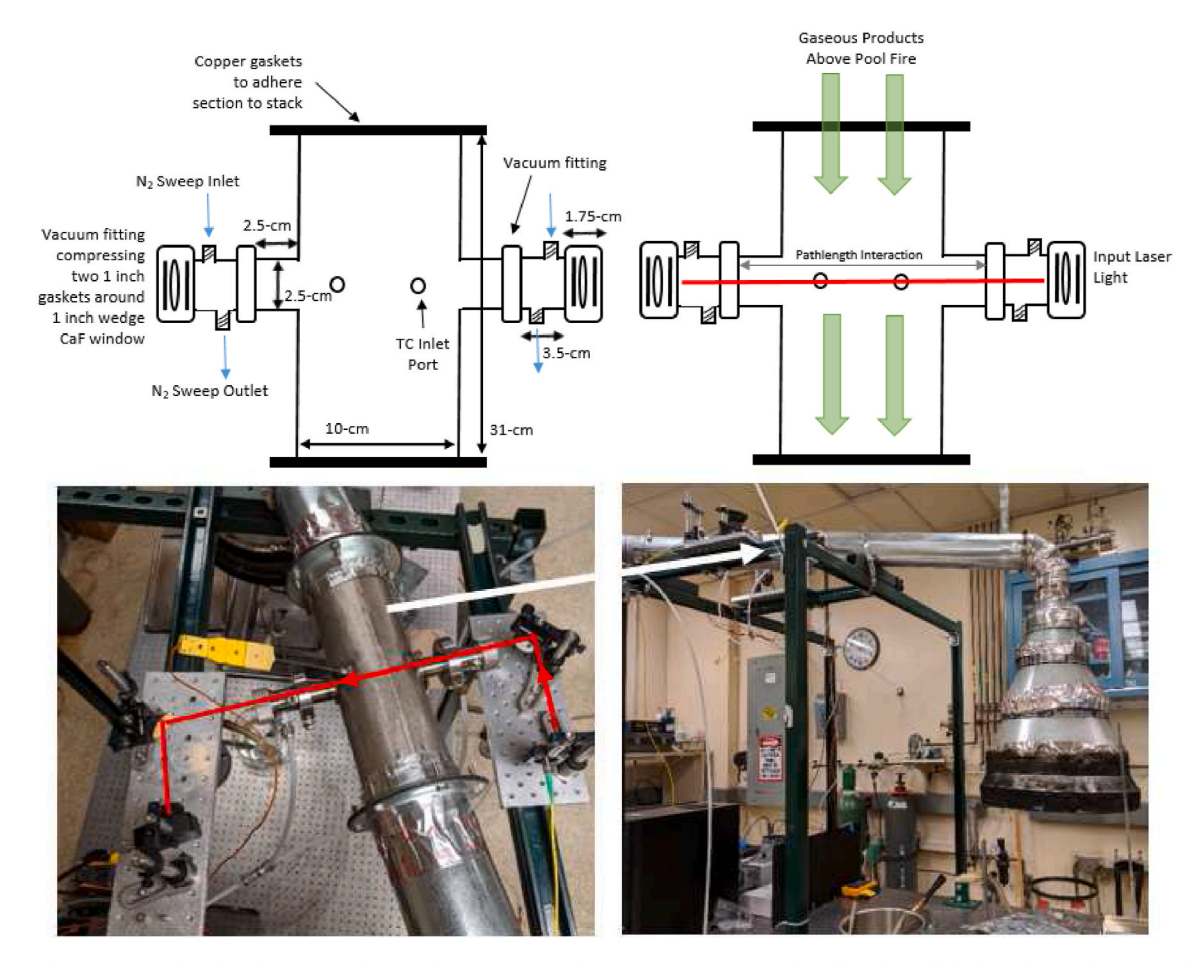


Fig. 1. (Top), schematic of modified stack section and example of experimental operation. (Bottom) Modified hood installed above the pool fire, optical train shown in red in the figure on the left (laser path from right to left). The white arrow between the figures denotes the position of the modified hood relative to the pool fire. (For interpretation of the references to color in this figure legend, the reader is referred to the Web version of this article.)

order to convert the output photocurrent signal to voltage. The  $\it trans$ -impedance amplifier was set to bias on DC current, full bandwidth (FBW), with a V/A of  $10^2$ .

## 2.2. Laser characterization

An Eblana 2.0 µm diode laser with current and temperature operating ranges of 0-120 mA and 0-50 °C respectively (EP2004-0-DM-B06-FM) was used to measure CO<sub>2</sub> concentration. The laser was mounted to a butterfly pin mount with temperature and current controls (ILX Lightwave, 9-PIN Female Current Control, 9-Pin Male Internal Temp Control). Laser temperature and current were controlled using an ILX controller (ILX Lightwave LDC-3714B). Laser wavenumber output was calibrated by setting a range of temperatures and currents and monitoring the output wavenumber of a Thermo Scientific Nicolet iS50 spectrometer. Calibration data for this laser has been published by Hinnant et al. [24]. Across a current range of 30-100 mA and a temperature range of 17-35 °C, the laser output wavenumber range was 4987.986–4994.058 cm<sup>-1</sup>. This range corresponds to the  $v_1+2v_2+v_3$ vibrational combination band for CO2 and includes 5 ro-vibrational transitions [25,26]. Data collected from HITRAN for the 5 absorption lines within the laser wavenumber range are presented in Table 1 [27]. v" and v' are the lower and upper vibrational transition states respectively, J" and J' are the lower and upper rotational transition states respectively,  $\tilde{v}$  is the wavenumber at which the transition occurs, S is the line strength (cm<sup>-1</sup>/molecule·cm<sup>2</sup>, for peak absorbance at 298K), ILX T and ILX mA are the temperature and current sets for said laser wavenumber output. In this work, CO2 absorbance was measured across the R

**Table 1**Parameters and laser settings describing the absorbing wavenumbers available within the laser temperature and current range measured.

		-						
Peak Number	ν"	$\nu'$	J″	$\mathbf{J}'$	ỹ (cm <sup>−1</sup> )	S	ILX T (°C)	ILX mA
1	0	2	14	15	4988.6547	1.31e- 21	35	55
2	0	2	16	17	4989.9714	1.32e- 21	29	95
3	0	2	18	19	4991.2584	1.29e- 21	25	74
4	0	2	20	21	4992.5156	1.23e- 21	21	70
5	0	2	22	23	4993.7431	1.15e- 21	17	61.5

(22) transition of the combination band, represented as the 5th peak in the table below.

#### 2.3. Materials

In this work, an emphasis was placed on studying materials likely to extinguish a heptane pool fire in order to observe differences in  ${\rm CO_2}$  profiles related to extinction. Given synergistic interactions reported by Ananth et al. [7], we examined mixtures of commercial siloxane surfactants and Glucopon 215 UP.

Mixture compositions were based on the RefAFFF formulation described by Hinnant et al. [28]. A 3:2 by weight ratio was maintained

between the siloxane surfactant and Glucopon 215 UP and included 0.5 wt% solvent (diethylene glycol butyl ether, DGBE). The total surfactant concentration was varied depending on the measured critical micelle concentration (CMC) of the mixture. Mixture concentrations were limited to less than 10 times CMC (the RefAFFF is at a concentration 10 times its CMC) and required a minimum surfactant concentration of 0.06 wt%, calculated from the surfactant concentrations reported in commercial products [29,30]. Mixture compositions are summarized in Table 2.

The siloxane surfactants evaluated included Dow-Corning, Inc. 67A, 501W, 502W, and 193A, Silwet L77 purchased from Momentive, Inc., and Gelest SiH 6185 purchased from Gelest Inc. (referred to in this report as Gel6185). Limited structural information is available for the commercial products from their safety data sheets [31-36]. 67A, Gel6185, and 502W are reported to have a trisiloxane tail structure and a polydisperse polyoxyethylene (PEO) head group, terminating in a hydroxyl group. L77 and 501W have a trisiloxane tail structure and polydisperse PEO head structure, and terminate in a methyl group. 193A has a polysiloxane tail and polydisperse PEO head group, terminating in a hydroxyl group. Variations in foam performance could therefore be due to differences in tail structure, PEO head length distribution, as well as terminating group. All of the mixtures contained Glucopon 215 UP (alkylpolyglycoside hydrocarbon surfactant purchased from BASF) and DGBE (purchased from Sigma Aldrich). The RefAFFF containing fluorinated surfactant Capstone 1157 N (provided by Chemours, Inc.) was also re-evaluated to determine its CO2 profile.

The mixtures were characterized through CMC, surface tension, interfacial tension with heptane, and foam expansion ratio. Structural differences between the surfactants are expected to produce differences in solution and foam properties, potentially resulting in extinction performance differences.

CMCs for the solutions were measured by varying the total surfactant concentration in an aqueous solution and measuring the surface tension. The concentration at the intersection of the linear surface tension range and the steady-state range was defined as the CMC. Surface tension and interfacial tension with heptane were measured using a Du Noüy ring tensiometer with a platinum iridium ring, 1 cm in diameter (Biolin Sigma 701 series). Foam expansion ratio (ER) was measured for foams generated during the fire extinction test, dividing a foam volume of 500 ml (measured in a beaker) by its weight (assuming a solution density of 1 g/ml). The ER is a measure of the foam liquid content: foams with smaller ERs have more water in their foam layer than foams with larger

## 3. Concentration calculations

Measured  $CO_2$  absorbance was used to calculate  $CO_2$  mole fraction through the Bouguer-Lambert Law in Equation (1), [37].

$$A = -\ln(\frac{I}{I_0}) = S_{v,T} g_{v,P,T} \rho_{P,T} \chi_i L$$
 (1)

A is absorbance, measured through a change in laser light intensity (I and I<sub>0</sub>). S is the line strength of the spectral feature (cm<sup>-1</sup>/molcm<sup>-2</sup>) and g is the line shape parameter (1/cm<sup>-1</sup>) [38], both at a specified wavenumber ( $\nu$ ), pressure (P), and temperature (T).  $\rho$  is the molecular density

(mol/cm [3], calculated from the ideal gas law),  $\chi_i$  is the mole fraction of  $CO_2$ , and L is the effective pathlength.

Absorbance was measured using a LabVIEW data acquisition system and processed with MATLAB. The CO<sub>2</sub> absorbing feature was defined by modulating the laser output wavenumber over a current range. The current was modulated as a saw-tooth waveform at a rate of 50 Hz and an applied amplitude of 3 V. A LabVIEW analog output voltage module (National Instruments NI 9264) acted as the waveform generator, connected to the ILX controller through a BNC cable. The ILX controller converted the waveform generator voltage into current at a transfer function of 10 mA/V. The ILX controller was set to 17  $^{\circ}$ C and 62 mA. For each saw-tooth waveform, the current output ranged from roughly 30-90 mA, corresponding to a laser wavenumber output range from 4994.058 to 4993.395 cm<sup>-1</sup>. This range is inclusive of one rotational transition, R(22), in the  $CO_2 v_1 + 2v_2 + v_3$  combination band. The detector signal and temperature were monitored using a LabVIEW analog input voltage module (National Instruments NI 9223) and an analog input temperature module (National Instruments NI 9211). Data was collected at a rate of 10,000 samples per second. This was below the sampling threshold of the voltage modules; however, the temperature module was only able to sample data at a rate of 1 S/s.

Data was exported from LabVIEW into an excel file that eliminated initial data points prior to the start of a sweep in the saw-tooth waveform. The data was then imported into MATLAB and extraneous data points that did not complete a full sweep were removed from the end of the set. The remaining data points were then categorized into individual sweeps and assessed for any erroneous data points possibly caused by passing soot particles. These individual points were removed from each sweep. 50 individual sweeps were then averaged to produce 1 sweep per second of data collection. A baseline 3rd order polynomial equation was then fit to each sweep to establish I<sub>0</sub>. CO<sub>2</sub> absorbance was then calculated by taking the natural log of the detector signal and the baseline fit for each data point in the sweep. Absorbance was plotted with laser output wavenumber, calculated using the measured voltage of the function generator, the ILX controller voltage to current ratio of 10 mA/ V, and the calibrated current to wavenumber curve for a set laser temperature of 17 °C shown in Equation (2).

$$Wavenumber = 2.049064*10^{-5}x^2 + 1.939832*10^{-3}x + 2.002305*10^3$$
 (2)

MATLAB was then used to fit the collected absorbance data to a model of the Bouguer-Lambert Law and solve for  $CO_2$  mole fraction. Line strength (S) and the line shape parameter (g) were defined using the HITRAN data base [23] over a range of temperatures and wavenumbers. The HAPI Python program [39] was used to access the HITRAN spectral database for the  $^{16}O^{12}C^{16}O$  isotopologue of  $CO_2$  over the wavenumber range 4993.2–4994.5 cm $^{-1}$ . Given the unavailability of parameters for  $CO_2$  at the desired wavenumbers for the Hartman-Tran line shape, the HAPI program defaulted to a Voigt line shape [40] to calculate line strength and line shape parameters for every  $0.001~cm^{-1}$  wavenumbers in the specified range, at intervals of every 1 K in the temperature range 280–840 K. The absorption coefficient values (line strength multiplied by line shape parameter) for the wavenumber range were stored in text files for the specified coded temperature. Text files were named 'CO2 300K', 'CO2 301K', and so forth.

To fit the data, temperature data was averaged across the 50 Hz to

Table 2
Weight% compositions of surfactant mixtures. "G215UP" refers to Glucopon 215 UP.

L77: G215	67A: G215	Gel6185: G215	501W: G215	502W: G215	193A: G215	Cap: G215
0.11% L77	0.06% 67A	0.06% Gel6185	0.04% 501W	0.08% 502W	0.3% 193A	0.3% Capstone
0.08% G215UP	0.04% G215UP	0.04% G215UP	0.03% G215UP	0.05% G215UP	0.2% G215UP	0.2% G215UP
0.5% DGBE	0.5% DGBE	0.5% DGBE	0.5% DGBE	0.5% DGBE	0.5% DGBE	0.5% DGBE

report 1 temperature per second of data collection. The integer temperature value was used to call the text file containing the absorption coefficient values across the specified wavenumber range. Using the calculated absorption coefficient values, a pathlength of 14 cm, a pressure of 1.001 atm, the temperature dependent molecular density, and an initial guess of  $\rm CO_2$  mole fraction, we modeled  $\rm CO_2$  absorbance for every second of data collection. The model was then compared to the collected absorbance data and the error between the two was minimized through MATLAB's "fmincon" function, based on a Nelder-Mead minimization. Error was minimized by iterating the mole fraction variable in the absorbance model. The LabVIEW, MATLAB, and Python programs used can be found in the Supplementary Section of this report.

To assess the accuracy of the MATLAB program, we fit the model to

known, measured concentrations of  $CO_2$  at room temperature. Before the modified hood was installed, the ends of the hood were sealed with tape and  $N_2$  and  $CO_2$  were fed through the sweep ports on one side. The ports on the other side of the hood were open to allow outflow. Gaseous flow rates were controlled with Alicat flow controllers (error in metered flow 0.6%) at flow rates representative of 3 different  $CO_2$  concentrations: 8, 4, and 1 mol%. Gases were fed into the hood for 30 min before sampling to ensure a steady-state concentration. Data was collected as specified above and processed using the MATLAB program at a constant room temperature (298K) with a modification to the pathlength. The calibrations did not use a  $N_2$  sweep, extending the full pathlength to the windows of the two hood ports, leading to a pathlength of 27.9 cm. The MATLAB program fit the 3 concentrations to values of 0.07019,

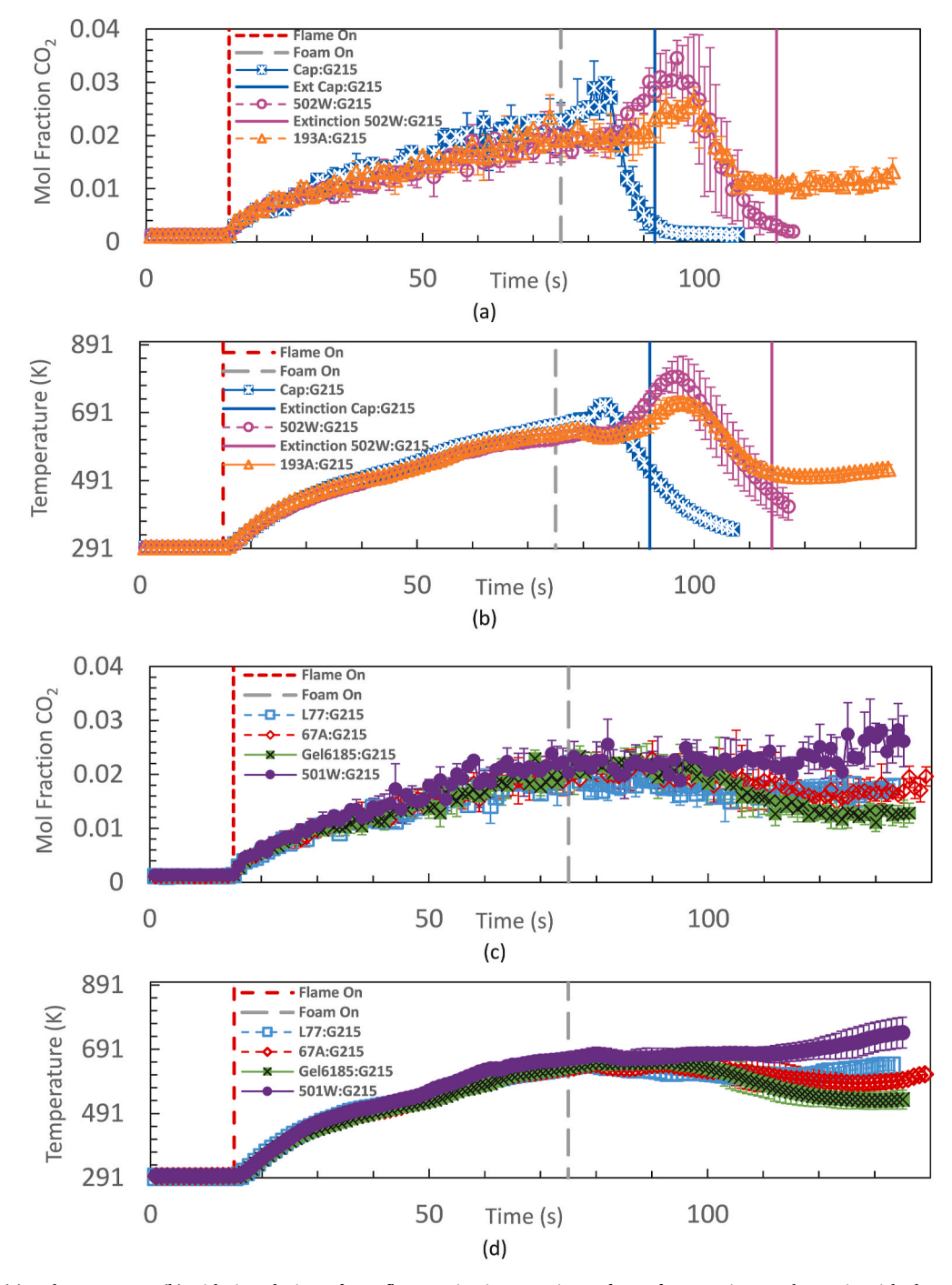


Fig. 2. CO<sub>2</sub> profile (a) and temperature (b) with time during a foam/flame extinction experiment for surfactant mixtures that extinguished or covered the fuel pool. CO<sub>2</sub> profile (c) and temperature (d) with time during foam/flame extinction experiment for surfactant mixtures that did not fully cover or extinguish the fuel pool.

 $0.03753,\, and\, 0.00993.$  This represents a percent error of  $13,\, 6,\, and\, 1\%$  for the  $8,\, 4$  and 1 mol% concentrations, all greater than the 0.6% error in Alicat flow rate, which appears to increase as the  $CO_2$  concentration increased.

#### 4. Results and discussion

The objective of this experiment was to differentiate extinction performance between firefighting foams at time-scales prior to extinction. Foams that quickly minimize  $\mathrm{CO}_2$  concentration reduce the burn rate of heptane and are considered more effective firefighting foams. Specific surfactant mixtures were chosen in an attempt to produce foams with a range in extinction performance that would show differences throughout the extinction experiment. We present and discuss the collected  $\mathrm{CO}_2$  profiles between the foams. Differences in profiles are linked to differences in surfactant structure and interactions between cosurfactants. Additionally, a limited set of surfactant dependent solution and foam properties are presented and discussed to determine if these properties trend with aspects of the  $\mathrm{CO}_2$  profiles.

#### 4.1. CO<sub>2</sub> profiles during foam application onto a heptane pool fire

Fig. 2(a) and Fig. 2(b) plot CO<sub>2</sub> concentration and temperature with time, respectively, during the foam fire extinction experiments for foams that fully covered the fuel pool and/or extinguished the pool fire. Fig. 2 (c) and (d) plot CO<sub>2</sub> concentration and temperature with time, respectively, during the foam fire extinction experiments for foams that did not fully cover the fuel pool or extinguish the fire. Data collection started 15 s before the fuel pool was ignited. The fuel pool was then ignited and allowed to preburn for 60 s. This preburn allowed the depth of the fuel pool to reach a steady-state temperature [41]. The vertical line "Flame On" denotes ignition. After the preburn, foam was applied to the pool surface, 75 s into data collection. The vertical line "Foam On" denotes the foam application start time. Profile differences after 75 s are expected for foams containing different surfactant mixtures. For foams that were able to extinguish the fire, a vertical line matching the color of the plotted foam profile is included to note extinction time. Error bars plotted represent two standard deviations calculated for three trials. Plots of CO2 profiles for each of the three trials for each foam can be found in the Supplementary Section of this report.

The  $\rm CO_2$  concentration and temperature profiles show good precision during the preburn between replicate trials, prior to foam application. After the preburn (after 75 s), deviations in the  $\rm CO_2$  and temperature profiles were observed based on differences in foam performance. Data collection and calculations show low error between trials and minimal noise between data points. The three trials of 502W: G215 showed the largest error during each stage of the experiment. During the background, preburn, and foam application stages, the three trials of 502W:G215 had an average percent error of 7.5, 12.6, and 29.5%. Considerably more noise is observed for the concentration data points compared to the temperature data points. This is due to the multistep calculation of individual concentration values versus the direct temperature measurement.

The TDLAS  $CO_2$  concentration results are encouraging as there does not appear to be a significant delay in detector response between pool ignition and increased  $CO_2$  concentration despite the physical distance between the pool and detector. This is not true of the temperature data which showed a 1-2 s lag between background and pool ignition. The temperature profiles are still comparative between surfactants in terms of the peak temperature achieved; however, data presented in subsequent tables have time stamps and values relative to the concentration profiles and not the temperature profiles. Of the seven foams tested, two extinguished a fire and three spread to cover the fuel pool. We first discuss the performance of the foams that could not cover the fuel pool or extinguish a fire, shown in Fig. 2(c) and (d).

Poor performance was observed for the L77, 67A, Gel6185, and

501W mixtures as none were able to extinguish the fire. Differences in their CO2 profiles were observed for comparative analysis. L77:G215 and 67A:G215 showed similarities through the entirety of the experiment. After foam application, a decrease in CO2 concentration to a steady-state mole fraction of roughly 0.017 was observed for both foams. This suggests that differences in structure between L77 and 67A have minor effects on interactions with G215 and do not contribute significantly to fire extinction performance. Gel6185:G215 reached a steady-state CO2 mole fraction of 0.013 which was lower than L77:G215 and 67A:G215 on average, but was within two standard deviations of their steady-state concentrations. The 501W:G215 foam showed the worst performance with a steady-state CO2 concentration that was statistically higher than the other foams after roughly 100 s. Despite no fire extinction for these four foams, the CO2 profiles show discrimination and suggest a ranking between these poor performing foams with performance improving from 501W:G215, L77:G215/67A:G215, to Gel6185:G215. The most noticeable differences in profile are only seen after roughly 25 s of foam application.

Foams that covered or extinguished the fuel pool, shown in Fig. 2(a) and (b), displayed unique profile characteristics compared to the foams that could not cover or extinguish the fire. 502W:G215, 193A:G215, and Cap:G215, the only foams to fully cover the fuel pool, were also the only foams with spikes in CO2 concentration after foam application. Temperature spikes were also observed which agrees with previous reports by Xu et al. [11] and Wang et al. [13]. Temperature spikes in those experiments were observed at a considerably later time, but this may be due to differences in agent application. Differences in time to peak CO2 value as well as peak CO2 value were also observed. We were also able to easily differentiate between foams that did and did not extinguish the fire. 502W:G215 and Cap:G215, the only 2 foams to extinguish the fire, were the only 2 foams to lower the CO2 mole fraction below 0.01. The CO2 profiles show steady-state behavior immediately following fire extinction. The extinction times for Cap:G215 and 502W:G215 were consistent with the extinction performance previously reported by Hinnant et al. [24] and Ananth et al. [7].

To elaborate on the observed  $CO_2$  peak, we present image stills during the foam fire extinction experiment for two foams that fully covered the fuel pool in Fig. 3.

At time 0, foam is deposited onto the center of the fuel pool. For capable foams, foam spreads over the fuel surface and fully covers the 19 cm diameter pool. This is achieved in under 10 s for the Cap:G215 foam and before 20 s for 502W;G215 and 193A;G215. Full pool coverage appears to create a more turbulent flame as seen comparing images at 10 s and 20 s for 193A:G215. We hypothesize that the profile spike is directly related to complete pool coverage and not simply introduction of foam onto the fuel pool. Only when the pool is fully covered, fuel gases are forced through pores or small openings within the foam layer. The pressure difference can lead to an increased flame speed, momentarily increasing the burn rate. After additional foam is applied, the flame is either extinguished or has reached a semi steady-state behavior. By 30 s, the 502W:G215 and 193A:G215 foam's have clearly reduced the flame height and visually, the flames appear very similar. From the profiles, this is seen as the decrease in CO2 concentration post-peak. For 193A:G215 at 30 s, the pool has become uncovered and foam recedes from the pool edges. The open pool is most clearly seen at the back of the pool, away from the camera on the right side of the image. This may explain why the 193A:G215 foam reached a steady-state concentration rather than continuing to minimize CO<sub>2</sub> concentration.

Without additional gaseous species detection and total exhaust  $\mathrm{CO}_2$  concentrations, we are unable to quantify HRR or describe the burn efficiency as foams are applied to a fire. However, the most important metric for fire suppression is the extinction time and measurements of  $\mathrm{CO}_2$  concentration appear to correlate with extinction performance. Pool fire extinction time corresponds to the time at which  $\mathrm{CO}_2$  concentration returns to a background concentration. We therefore have confidence that at times before extinction, the  $\mathrm{CO}_2$  concentration can be

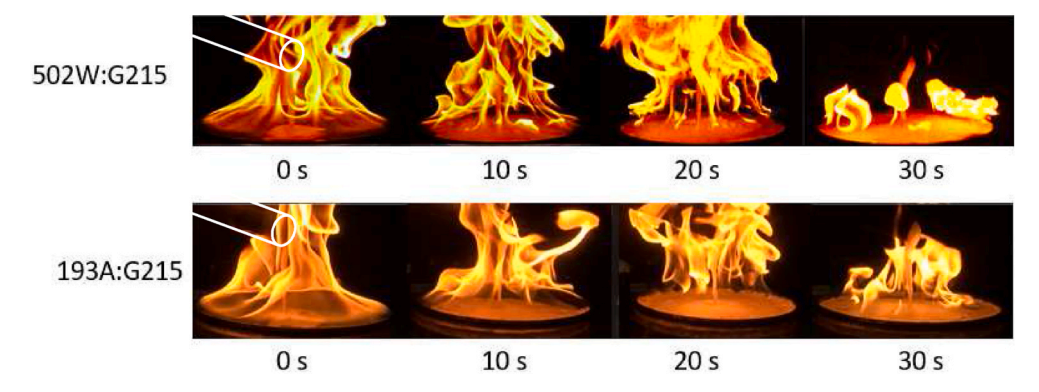


Fig. 3. Time lapsed images of 502W:G215 (top) and 193A:G215 (bottom) foams dispensed over a heptane pool fire. Foam is dispensed at the pool center from a 2.5 cm diameter charred glass tube.

used to describe extinction behavior. Additional gaseous detection should be explored for foam/fire systems to define burn efficiency and HRR; however,  $CO_2$  measurement with time alone may be sufficient to differentiate extinction performance between firefighting foams.

Data observed from the fire extinction tests (pool coverage time and extinction time) as well as new metrics gleamed from the  $\text{CO}_2$  profiles (time to peak  $\text{CO}_2$  value and peak  $\text{CO}_2$  value) are summarized in Table 3. We also report the  $\text{CO}_2$  concentration at the time of extinction or the steady-state  $\text{CO}_2$  concentration from foams that did not extinguish the fire. We suggest that these new metrics may trend with fire extinction performance and could potentially be used to indicate important time-scales for foam fire suppression. These new metrics may also be related to differences in foam surfactant composition.

Table 3 also reports measured foam flow rate between foams. Foam flow rates for foams that did not extinguish range from 1214 to 1308 ml/min while the range for foams that did extinguish are slightly higher, 1482 and 1569 ml/min. The Cap:G215 foam at a 1482 ml/min flow rate extinguished 20 s faster than the 502W:G215 foam at 1569 ml/min. Additionally, the 193A:G215 was able to cover a fuel pool with a foam flow rate of 1245 ml/min, similar to the flow rates of other trisiloxane mixtures. We do not believe these small differences in foam flow rate are contributing to significant differences in foam spreading or extinction performance.

Cap:G215 has the fastest pool coverage time, time to peak  $CO_2$  value, and extinction time. This suggests a potential trend between coverage time and time to peak  $CO_2$  value to extinction. For the two foams that

**Table 3** Metrics from the CO<sub>2</sub> extinction profiles.

Foam	Foam Flow Rate (mL/ min)	Pool Coverage Time (s)	Time to Peak CO <sub>2</sub> (s)	Peak CO <sub>2</sub> Value (x <sub>i</sub> )	CO <sub>2</sub> Steady- State or Extinction Value (x <sub>i</sub> )	Extinction Time (s)
L77: G215 Gel6185:	$1214 \pm 45 \\ 1226$	No Coverage No	N/A N/A	N/A N/A	0.017 0.013	No Extinction No
G215 67A: G215	$\begin{array}{c} \pm\ 16 \\ 1308 \\ \pm\ 13 \end{array}$	Coverage No Coverage	N/A	N/A	0.017	Extinction No Extinction
501W: G215	1297 ± 20	No Coverage	N/A	N/A	0.026	No Extinction
502W: G215	1569 ± 94	$14\pm 2$	21 ± 3	$0.037 \pm 0.002$	0.0037	$36\pm3$
193A: G215	$\begin{array}{c} 1245 \\ \pm \ 8 \end{array}$	$16\pm1$	$\begin{array}{c} 21 \; \pm \\ 4 \end{array}$	$0.028 \pm 0.002$	0.012	No Extinction
Cap: G215	$\begin{array}{c} 1482 \\ \pm \ 10 \end{array}$	4 ± 1	$8\pm2$	$\begin{array}{c} 0.031 \\ \pm \\ 0.002 \end{array}$	0.0052	$16\pm3$

extinguished a fire, their coverage times represent less than half of the full extinction event and the time to peak  $\rm CO_2$  represents 58% and 50% of the extinction event for 502W:G215 and Cap:G215 respectively. Mechanisms of foam fire suppression that act at short time-scales may be relevant to fire extinction if a correlation can be shown between coverage time, time to peak  $\rm CO_2$ , and extinction.

However, interesting metrics are seen between 502W:G215 and 193A:G215, one of which extinguished the fire while the other did not. We see almost identical  ${\rm CO_2}$  profiles until 108 s into the experiment. Between roughly 100 and 108 s, the foams have identical rates of  ${\rm CO_2}$  minimization. After this time, the 502W:G215 foam continues to minimize  ${\rm CO_2}$  concentration and maintains coverage of the fuel pool. Alternatively, the 193A:G215 foam begins to recede from the pool surface and reaches a steady-state concentration. The two foams have statistically similar coverage times and time to peak  ${\rm CO_2}$  value, but differ in peak  ${\rm CO_2}$  value. Differences are most noticeably observed at times close to the extinction event.  ${\rm 502W:G215}$  extinguishes the fire in 36 s (111 s in the plots above). Deviations between the  ${\rm 502W:G215}$  and  ${\rm 193A:G215}$  profiles are only seen in the last 3 s of the  ${\rm 502W:G215}$  extinction time. This limited comparison suggests that foam fire extinction mechanisms that impact longer time-scales may be relevant to fire extinction.

Although this limited series demonstrates the potential for new metrics and comparisons between foams using a  $\rm CO_2$  TDLAS experiment above a pool fire, not enough data was collected to make definitive claims between profile metrics, important time-scales, and extinction performance. We only observed two examples of foam fire extinction out of a set of seven foams. Although commercial products contain proprietary formulations, Snow et al. [42] demonstrated their ability to extinguish a 19 cm heptane pool fire. Additional profiles for foams that extinguish a fire are vital to determine whether short or long time-scales are important for differentiating firefighting performance. Continued testing will provide necessary examples of foam fire extinction for quantitative relationships to be developed between  $\rm CO_2$  profiles metrics and extinction.

## 4.2. Solution and foam properties

We suspect surfactant structural effects influence extinction and may be related to solution or foam properties. Therefore, a limited set of solution and foam properties were measured to characterize the materials studied and we discuss whether these properties trend with extinction performance or metrics from the  $\rm CO_2$  profiles. Table 4 reports solution CMC, surface tension, interfacial tension with heptane, and foam expansion ratio.

The three foams with the largest CMC values were the only foams to fully cover the fuel surface; however, there is not a quantitative trend between CMC, coverage time, or extinction time. L77:G215 and 67A: G215 showed similar performance (no extinction, steady-state  $\rm CO_2$  mole fraction of 0.017) and have similar CMC values. 501W:G215 and

**Table 4**Measured solution and foam properties for the 7 foam mixtures analyzed in this report. Surface tension and interfacial tension error are 0.5 mN/m for all solutions.

Mixture Solution	CMC (wt %)	Surface Tension (mN/m)	Interfacial Tension Heptane (mN/m)	Foam Expansion Ratio
L77:G215	$\begin{array}{c} \textbf{0.022\%} \; \pm \\ \textbf{0.003\%} \end{array}$	19.69	8.22	$9.5 \pm 0.6$
67A:G215	$\begin{array}{c} 0.019\% \; \pm \\ 0.003\% \end{array}$	20.09	6.42	$\textbf{8.7} \pm \textbf{0.1}$
Gel6185: G215	$\begin{array}{c} 0.011\% \; \pm \\ 0.001\% \end{array}$	19.43	6.38	$8.9 \pm 0.1$
501W: G215	$0.010\% \pm 0.001\%$	19.87	12.33	$7.0 \pm 0.3$
502W: G215	0.030% ± 0.004%	21.36	3.27	$\textbf{6.3} \pm \textbf{0.8}$
193A: G215	0.051% ± 0.006%	28.90	7.17	$7.6 \pm 0.3$
Cap:G215	0.079% ± 0.015%	16.70	1.93	$4.6\pm0.1$

Gel6185:G215 also have similar CMC values, but showed significant differences in their ability to minimize  $\rm CO_2$  concentration with time (0.026 and 0.013 respectively). Structural differences between Gel6185 and 501W are not contributing to differences in CMC, but are effecting extinction performance.

The mixtures demonstrate surface tension values characteristic of the siloxane or fluorocarbon component. A solution of 0.5% G215 had a surface tension of 31.1 mN/m (Hinnant et al. [20]). There are significant similarities between the trisiloxane mixture surface tensions while 193A:G215 shows a larger value and Cap:G215 has the smallest value. 193A has a polysiloxane tail structure which appears to be contributing to a difference in surface tension and CMC. The similarities in surface tension value between 502W:G215 and the other trisiloxane mixtures do not explain its superior fire extinction capability.

The greatest property variation is seen in solution interfacial tension with heptane. 502W:G215 and Cap:G215 have the two lowest values and are the only two foams to extinguish the fuel pool. 501W:G215 has the largest interfacial tension with heptane and demonstrated the poorest performance of the seven foams. From this limited data set, interfacial tension appears to trend with extinction performance; however, it does not account for the pool coverage differences between 193A:G215 and the other trisiloxane mixtures. Additional examples of foams that extinguish a fire with variation in interfacial tension are necessary to define this potential trend.

ER does not appear to trend with extinction performance. Cap:G215 has the fastest extinction and the lowest expansion ratio. However, 501W:G215, 502W:G215, and 193A:G215 have statistically similar expansion ratios, but one is able to extinguish a fire while two are not.

## 5. Conclusion

A  $\rm CO_2$  TDLAS experiment was designed to monitor foam fire extinction throughout an extinction experiment. We hypothesized that performance differences may be observed at important time-scales relevant to different mechanisms of foam fire extinction. By defining these time-scales, we may identify a mechanism of foam fire suppression important to rapid fire extinction. Trends could then be developed between this mechanism and different surfactant structures in order to develop optimized structures for rapid fire suppression. Our study focused on 6 siloxane surfactant mixture containing foams and a fluorinated surfactant mixture foam for comparison.

The modified hood design, LabVIEW data acquisition system, and MATLAB processing program were successful in calculating  $\mathrm{CO}_2$  profiles for the seven surfactant mixture foams analyzed in this report. Concentration profiles showed very little response lag between the 19 cm

heptane pool fire experiment and hood above the pool fire. Consistency was seen between background  ${\rm CO_2}$  concentrations, the preburns, and between the three trials of each foam.

Comparison of profiles led to discriminating performance differences between five of the foams that were unable to extinguish the fuel pool. 501W:G215 showed an increase in CO $_2$  concentration with time throughout the entire experiment. L77:G215 and 67A:G215 both lowered CO $_2$  concentrations, but not as quickly as Gel6185:G215 or 193A: G215. The foams that minimized CO $_2$  concentrations the most were the two foams that extinguished the fire: 502W:G215 and Cap:G215. Single gaseous species detection is not sufficient to further describe the HRR or burn efficiency of the flames being extinguished, and O $_2$  and CO should be considered in future analysis. However, the data presented suggest that detection of CO $_2$  can differentiate firefighting extinction potential among fire suppressing foams containing different surfactant formulations.

For foams that were able to cover or extinguish the fuel pool, we observed peaks in CO<sub>2</sub> concentration post pool coverage that seem to be related to an increase in flame turbulence as foam completely covers the pool fire. We observed three cases of pool coverage and two cases of full fire extinction. Cap:G215 demonstrated the fastest pool coverage times, time to peak CO<sub>2</sub> value, and extinction time. This suggests mechanisms that occur at short time-scales during foam fire extinction may be important to rapid fire suppression. However, 502W:G215 and 193A: G215 showed similar coverage time and time to peak CO<sub>2</sub> value and their profiles only diverged at time-scales close to final extinction. This suggests the importance of mechanisms occurring at later time-scales. Given the small sample size, we are unable to make definitive claims.

Little differences were seen in solution and foam properties between the trisiloxane surfactant mixtures despite 502W:G215 extinguishing the pool fire while the four others could not. There appears to be a slight trend between interfacial tension with heptane and extinction performance. This property should be evaluated further in trying to understand its connection to fire extinction and its connection to surfactant structural elements.

#### Author statement

Katherine Hinnant: Conceptualization, Methodology, Software, Validation, Formal analysis, Investigation, Writing-Original Draft, Writing- Review & Editing, Spencer Giles: Investigation, Resources, Writing- Original Draft, Writing- Review & Editing, Ramagopal Ananth: Conceptualization, Investigation, Writing- Original Draft, Writing- Review & Editing, Supervision, Project administration, Funding acquisition, J. Houston Miller: Conceptualization, Methodology, Software, Writing-Original Draft, Writing- Review & Editing, Supervision, Project administration.

### Declaration of competing interest

The authors declare that they have no known competing financial interests or personal relationships that could have appeared to influence the work reported in this paper.

#### Acknowledgement

We are thankful for financial support from the Naval Research Laboratory through the Edison Memorial Graduate Training Program, the Office of Naval Research (ONR), and from program manager Dr. Robin Nissan, Strategic Environmental Research and Development Program (SERDP) of U.S. Department of Defense (DOD) under WP-2739, WP18-1592, and WP20-1507.

## Appendix A. Supplementary data

Supplementary data to this article can be found online at https://doi.

org/10.1016/j.firesaf.2021.103488.

#### References

- [1] Co-operation of existing chemicals hazard assessment of perfluorooctane sulfonate (PFOS) and its salts, in: Environment Directorate Joint Meeting of the Chemicals Committee and the Working Party on Chemicals, Pesticides, and Biotechnology. ENV/JM/RD(2002)17/FINAL, 2002.
- [2] K.A. Barzen-Hanson, S.C. Roberts, S. Choyke, K. Oetjen, A. McAlees, N. Riddell, R. McCrindle, P.L. Ferguson, C.P. Higgins, J.A. Field, Discovery of 40 classes of perand polyfluoroalkyl substances in historical aqueous film-forming foams (AFFFs) a d AFFF-impacted groundwater, Environ. Sci. Technol. 51 (2017) 2047-2057.
- [3] N.M. Kovalchuk, A. Trybala, V. Starov, O. Matar, N. Ivanova, Fluoro- vs hydrocarbon surfactants: why do they differ in wetting performance? Adv. Colloid Interface Sci. 210 (2014) 65-71.
- R.L. Tuve, H.B. Peterson, E.J. Jablonski, R.R. Neill, A New Vapor-Securing Agent for Flammable-Liquid Fire Extinguishment, U.S. Naval Research Laboratory Report 6057, DTIC Document No. ADA07449038, Washington DC, March 13, 1964.
- [5] R.H. Hetzer, F. Kümmerlen, K. Wirz, D. Blunk, Fire testing a new fluorine-free AFFF based on a novel Class of environmentally sound high performance siloxane surfactants, in: Fire Safety Science Proceedings of the 11th International
- Symposium, 2014, pp. 1261–1270. Y. Sheng, Q. Wang, Y. Zhao, X. Liu, Study of environmentally-friendly firefighting foam based on the mixture of hydrocarbon and silicone surfactants, Fire Technol. 56 (2020) 1059-1075.
- R. Ananth, A.W. Snow, K.M. Hinnant, S.L. Giles, J.P. Farley, Synergisms between siloxane-polyoxyethylene and alkyl polyglycoside surfactants in foam stability and pool fire extinction, Colloids Surf., A 579 (2019) 123686.
- [8] R. Ananth, K.M. Hinnant, S.L. Giles, J.P. Farley, A.W. Snow, Environmentally-Friendly Surfactants for Foams with Low Fuel Permeability Needed for Effective Pool Fire Suppression, vol. 145, U.S. Naval Research Laboratory Memorandum Report, Washington, D.C., 2020. NRL/MR/6180-20-10145, https://apps.dtic.mil/ sti/citations/AD1111148.
- [9] S.A. Magrabi, B.Z. Dlugogorski, G.J. Jameson, A comparative study of drainage characteristics in AFFF and FFP compressed-air fire-fighting foams, Fire Saf. J. 37
- [10] K.M. Hinnant, R. Ananth, J.P. Farley, C.L. Whitehurst, S.L. Giles, W.A. Maza, A. W. Snow, S. Karwoski, Extinction Performance Summary of Commercial Fluorinefree Firefighting Foams over a 28 Ft2 Pool Fire Detailed by MIL-PRF-24385, U.S. Naval Research Laboratory Memorandum Report, Washington, D.C., 2020. NRL/ MR/6185—20-10031, https://apps.dtic.mil/sti/citations/AD1100426.
- [11] Z. Xu, X. Guo, L. Yan, W. Kang, Fire-extinguishing performance and mechanism of aqueous film-forming foam in diesel pool fire, Case Stud. Thermal Eng. 17 (2020) 100578.
- [12] D. Rie, J. Lee, S. Kim, Class B fire-extinguishing performance evaluation of a compressed air foam system at different air-to-aqueous foam solution mixing ratios, Appl. Sci. 6 (191) (2016), https://doi.org/10.3390/app6070191.
- [13] K. Wang, J. Fang, H.R. Shah, S. Mu, X. Lang, J. Wang, Y. Zhang, A theoretical and experimental study of extinguishing compressed air foam on an n-heptane storage fire with variable fuel thickness, Process Saf. Environ. Protect. 138 (2020) 117\_129
- [14] C. Huggett, Estimation of rate of heat release by means of oxygen consumption neasurements, Fire Mater. 4 (2) (1980) 61-65.
- V. Babrauskas, Development of the cone calorimeter- A bench-scale heat release ite apparatus based on oxygen consumption, Fire Mater. 8 (2) (1984) 81-95.
- [16] J. Martinka, T. Chrebet, K. Balog, An assessment of petrol fire risk by oxygen consumption calorimetry, J. Therm. Anal. Calorim. 117 (2014) 325-332.
- [17] B.Z. Dlugogorski, J.R. Mawhinney, V. Huu Duc, The measurement of heat release rates by oxygen consumption calorimetry in fires under suppression, Fire Saf. Sci. 4 (1994) 877-888.
- [18] D.M. Bailey, E.A. Adkins, J.H. Miller, An open-path tunable diode laser absorption spectrometer for detection of carbon dioxide at the Bonanza Creek Long-Term Ecological Research Site near Fairbanks, Alaska, Appl. Phys. B 123 (2017) 245.
- [19] Y. Hu, S. Naito, N. Kobayaski, M. Hasatani, CO2, NOx, and SO2 emissions from the combustion of coal with high oxygen concentration gases, Fuel 79 (2000) 1925-1932.
- R.M. Mihalcea, D.S. Baer, R.K. Hanson, Advanced diode laser absorption sensor for in situ combustion measurements of CO2, H2O and gas temperature, in:

- Proceedings 27th International Symposium for the Combustion Institute, 1998, pp. 95-101.
- [21] X. Zhu, S. Yao, W. Ren, Z. Lu, Z. Li, TDLAS monitoring of carbon dioxide with temperature compensation in power plant exhausts, Appl. Sci. 9 (442) (2019).
- [22] M.E. Webber, K. Suhong, S.T. Sanders, D.S. Baer, R.K. Hanson, Y. Ikeda, In situ combustion measurements of CO2 by use of a distributed-feedback diode-laser ensor near 2.0 µm, Appl. Opt. 40 (6) (2001) 821–828.
- [23] E.A. Fallows, T.G. Cleary, J.H. Miller, Development of a multiple gas analyzer using cavity ringdown spectroscopy for use in advanced fire detection, Appl. Opt. 48 (4) (2009) 695-703.
- K.M. Hinnant, Characterizing Trends between Surfactant Structure, Fuel Transport through a Foam Layer, and Foam Fire Extinction Performance for Firefighting Foams Containing Novel Environmentally-Friendly Surfactants (ID 15494), Doctoral dissertation, George Washington University]. ProQuest Dissertations Publishing, 2021.
- [25] P.A. Gerakines, J.J. Bray, A. Davis, C.R. Richey, The strengths of near-infrared absorption features relevant to interstellar and planetary ices, Astrophys. J. 620 (2005) 1140-1150.
- [26] E. Quirico, B. Schmitt, Near-infrared spectroscopy of simple hydrocarbons and carbon oxides diluted in solid N2 and as pure ices: implications for triton and pluto, Icarus 127 (1997) 354-378.
- [27] I.E. Gordon, L.S. Rothman, C. Hill, R.V. Kochanov, Y. Tan, P.F. Bernath, M. Birk, V. Boudon, A. Campargue, K.V. Chance, B.J. Drouin, J.M. Flaud, R.R. Gamache, J. T. Hodges, D. Jacquemart, V.I. Perevalov, A. Perrin, K.P. Shine, M.A.H. Smith, J. Tennyson, G.C. Toon, H. Tran, V.G. Tyuterev, A. Barbe, A.G. Császár, V.M. Devi, T. Furtenbacher, J.J. Harrison, J.M. Hartmann, A. Jolly, T.J. Johnson, T. Karman, I. Kleiner, A.A. Kyuberis, J. Loos, O.M. Lyulin, S.T. Massie, S.N. Mikhailenko, N. Moazzen-Ahmadi, H.S.P. Müller, O.V. Naumenko, A.V. Nikitin, O.L. Polyansky, M. Rey, M. Rotger, S.W. Sharpe, K. Sung, E. Starikova, S.A. Tashkun, J.V. Auwera, G. Wagner, J. Wilzewski, P. Wcisło, S. Yu, E.J. Zak, The HITRAN2016 molecular ectroscopic database, J. Quant. Spectrosc. Radiat. Transf. 203 (2017) 3-69.
- [28] K.M. Hinnant, S.L. Giles, A.W. Snow, J.P. Farley, J.W. Fleming, R. Ananth, An analytically defined fire-suppressing foam formulation for evaluation of fluorosurfactant replacement, J. Surfactants Deterg. (2018), https://doi.org/ 10.1002/jsde.12166.
- [29] National foam, "aer-O-LiteTMC6 3% aqueous film forming foam", in: NMS#300 safety data sheet 2, 2016, November,
- [30] Buckeye fire equipment company, "buckeye 3% MIL SPEC AFFF", in: material safety data sheet 11, 2012. January.
- Gelest, "SIH6185.0- 3-[HYDROXY(POLYETHYLENEOXY)PROPYL]-
- HEPTAMETHYLIRISILOXANE, 90%", Version 1.0, November, 20, 2014.

  [32] Dow Corning®, "Dow Corning 502W Additive", 1211141-00007 SDS Number, Version 2.1, Nov. 2015 [Revised November, 1, 2016].
- [33] Dow®, DOWSIL™ 67 additive, safety datasheet, February 11 (2018).
- [34] Mometive™, "Silwet L-77" Safety Data Sheet, Version 1.15, 2017, 12,4.
   [35] Dow®, Product name: DOWSIL™ 501W additive, in: safety data sheet 14, 2018.
- February.
- Dow®, Product name: VORASURF™ DC 193 additive, in: safety data sheet 8, 2020. [36]
- [37] D.H. Plemmons, N.A. Galyen, W.J. Phillips, B.C. Winleman, Measurements of line strength and line shape parameters of the HCl R3 (02) 5739.263 cm-1 and HF R1 (0-2) 7823.820 cm-1 transitions, J. Phys.: Conf. Series XXII Int. Conf. Spectral Line Shapes 2014 548 (2014), 012019.
- [38] Calculation of molecular spectra with the Spectral Calculator. Calculating Gas Spectra. www.spectralcalc.com. Accessed Aug 9, 2021. https://www.spectralcalc. com/info/CalculatingSpectra.pdf.
- R.V. Kochanov, I.E. Gordon, L.S. Rothman, P. Wcislo, C. Hill, J.S. Wilzewski, HITRAN Application Programming Interface (HAPI): a comprehensive approach to working with spectroscopic data, J. Quant. Spectrosc. Radiat. Transfer 177 (2016)
- [40] N.H. Ngo, D. Lisak, H. Tran, J.M. Hartmann, An isolated line-shape model to go beyond the Voigt profile in spectroscopic databases and radiative transfer codes, J. Quant. Spectrosc. Radiat. Transfer 129 (2013) 89–100.
- [41] M.W. Conroy, J.W. Fleming, R. Ananth, Surface cooling of a pool fire by aqueous foams, Combust. Sci. Technol. 189 (2017) 806-840.
- [42] A.W. Snow, S. Giles, K. Hinnant, J. Farley, R. Ananth, Fuel for Firefighting Foam Evaluations: Gasoline vs Heptane, U.S. Naval Research Laboratory Memorandum Report, Washington, D.C., 2019. NRL/MR/6123—19-9895, https://apps.dtic.mil/ sti/citations/AD1076690.